

Lattice modulus and crystallite thickness measurements in ultra-high modulus linear polyethylene*

J. Clements, R. Jakeways and I. M. Ward

Department of Physics, University of Leeds, Leeds LS2 9JT, UK
(Received 12 December 1977)

Measurements have been made of the apparent Young's modulus of the crystalline part of a number of ultra-high modulus polyethylene drawn tapes by observing the change in Bragg angle of the 002 X-ray reflection when the tapes are placed under stress. The variation with temperature has been measured and it is argued that the common limiting value of modulus reached by all samples at low temperature represents the true crystalline modulus and that the room temperature value, which is some 40% lower, is strongly suggestive of a morphology in which a considerable fraction of the material is non-crystalline and is located, from the mechanical point of view, essentially in parallel with the crystalline fraction. Accurate measurements of the linewidths of the 200, 020 and 002 X-ray reflections have been made in order to deduce the mean thickness of the crystalline elements in the three principal directions. The 'a' and 'b' thicknesses vary very little with draw ratio but the 'c' thickness increases at high draw ratios to a value more than twice as great as the (constant) long period determined from small-angle scattering.

INTRODUCTION

The morphology of ultra-high modulus linear polyethylene fibres¹⁻³ is of considerable interest from the point of view of relating the mechanical properties of these materials to their structure. We have used X-ray techniques to learn something of the distribution and orientation of the crystalline fractions of the fibres and the deductions made are used in another publication⁴ which attempts to model the material using a statistical model in which the mechanical modulus is related to the degree of crystal continuity introduced by the presence of intercrystalline bridges. It should be pointed out immediately that it is very important to define clearly what one means by crystalline in the polymer context. To an X-ray crystallographer the crystalline state implies a region of sufficient size to give reasonably sharp X-ray reflections. Typically these will be from 0.5° to 2° wide (measured in 2θ) and thus arise from scattering units having crystalline continuity over a range of 50 Å or greater. Other techniques which are sensitive to crystallinity may recognize much smaller regions as being crystalline. Hence, independent measures of crystallinity are liable to disagree with one another, perhaps substantially.

We have measured the apparent crystal modulus of the fibres (defined as the ratio of bulk stress to crystalline strain) over a wide range of temperatures on samples of differing draw ratio and molecular weight. The results give us these basic pieces of information: (a) an upper limit for the crystalline fraction; (b) the ultimate true crystalline modulus; (c) a guide to the way in which crystalline material is distributed throughout the material.

We have also measured the mean thicknesses of the crystalline regions in three orthogonal directions and the

measurements give further pointers to the morphology of the specimen.

Small-angle X-ray measurements have also been carried out to determine the dimensions of the lamellar structure which persists, albeit weakly, even in the highest draw ratio specimens.

EXPERIMENTAL

Sample preparation

The materials investigated were three grades of linear polyethylene (LPE) (BP Chemicals International): HO20-54P, $\bar{M}_w = 312\,000$, $\bar{M}_n = 33\,000$ (sample 1); Rigidex 50, $\bar{M}_w = 101\,450$, $\bar{M}_n = 6060$ (sample 2); Rigidex 9, $\bar{M}_w = 126\,600$, $\bar{M}_n = 6060$ (sample 3).

Isotropic sheets 0.5–0.7 mm thick were prepared by compression moulding the pellets (powder) of polymer at 160°C between copper plates, and then quenching in cold water. Dumb-bell specimens of 20 mm gauge length were then cut and drawn in air at different temperatures in an Instron tensile testing machine, using a crosshead speed of 100 mm/min.

The specimens tested were all in the form of tapes of cross-section approximately 1.0 × 0.1 mm and about 40 mm in length.

A few samples of Rigidex 50 were also produced for crystal thickness measurements only, by hydrostatic extrusion, as described in the related publication⁴.

Crystal strain measurements

A Siemens K-4 X-ray set and a type F diffractometer employing nickel-filtered CuK α radiation was used for the measurement of lattice extension under stress. The specimens were mounted horizontally in the stretching rig, which

* Presented at the Polymer Physics Group (Institute of Physics) Biennial Conference, Shrivenham, September 1977.

was designed to fit on the diffractometer table. The rig was constructed so that a load of several kilograms could be applied axially to the specimens, without altering their position.

The basic technique of the X-ray measurements was to determine the Bragg angle of the (002) reflections as a function of the applied load. Changes which occurred were typically of the order of 0.1%, i.e. changes in 2θ of less than 0.1° , which compares unfavourably with the natural linewidth of 0.2° – 0.5° .

Fluctuations in the direction of the primary beam which arose during the course of protracted measurements were found to lead to apparent changes in the Bragg angle of the same order as that which would arise from straining the specimen. A technique was devised to overcome this problem, and has been described in detail elsewhere⁵.

A series of loads was used for each of the specimens and the lattice strain determined, being equal to $-\cot\theta d\theta$.

In all cases, the deformation was found to be elastic and immediate; time dependent effects, such as are found in mechanical measurements were not observed. The recovery on removal of the load was also found to be immediate and complete.

A graph of lattice strain *versus* applied stress immediately produces a value for the apparent modulus, making the initial assumption of homogeneous stress in the specimen.

For the measurement of moduli below room temperature a small enclosure of rigid polyurethane foam was built, which, when mounted around the specimen, could be flushed with cold nitrogen gas. This arrangement allowed measurements between room temperature and $\sim -170^\circ\text{C}$ to be performed. It was found that the enclosure caused a 20% reduction in the peak intensity but no other significant effects were observed.

No measurements were made on the extruded materials.

Measurements of mean crystal thickness

Crystallite size studies have been made on the samples by direct evaluation of the crystallite dimensions from the broadening observed in the wide-angle X-ray scattering.

The (200), (020), and (002) reflections were scanned on the Siemens X-ray diffractometer under high resolution conditions (about 0.1° or less in 2θ). A scintillation counter was used with a pulse height discriminator to detect the scattered radiation.

The counting time was chosen so as to accumulate a few thousand counts at the peak maximum and was typically 10–100 sec, and the recording interval was 0.02° in 2θ . The observed profiles were corrected for instrumental and $K\alpha$ doublet broadening by means of Stokes' method⁶. The method requires a profile of a standard substance of 'powder' morphology consisting of such large crystallites that the inherent line broadening due to the specimen is negligible compared with instrumental broadening. The standards chosen were aluminium and gold in suitable form for mounting on the diffractometer.

In the measurements of the profiles, the following procedure was adopted with the samples. In the case of the (200) and (020) reflections, profiles were observed with the 'reflection' arrangement. In the case of the (002) reflection profiles were recorded in 'transmission'. In all cases it was found necessary to apply a small strain ($\sim 0.025\%$) to the samples, in order to keep them straight.

The range of measurement in 2θ was extended to about five times the full width at half maximum on both sides of

the peak. The narrow angular range involved eliminated the necessity for Lorentz polarization and temperature corrections.

Crystal thicknesses were derived from the line shapes of appropriate X-ray reflections, the integral breadth (= line area/height) being the parameter used.

Various relationships have been quoted to relate linewidth (or integral breadth) to crystallite size, all being based on the simple idea of the finite resolving power of a diffraction grating. A typical quoted relationship is:

$$D_{hkl} = \frac{\lambda f}{\cos\theta \Delta(2\theta)}$$

where D_{hkl} is the thickness of diffracting elements normal to the hkl plane; λ is the X-ray wavelength; 2θ is the Bragg angle; f is a number close to 1 and $\Delta(2\theta)$ is the linewidth.

In the polymer case we will not in general find a unique value of D and we are thus concerned to derive an average value, \bar{D} . A simple analysis demonstrates that the integral breadth gives a true mean value for D_{hkl} and computer simulations of diffraction lines gave a value for f close to 0.9 for a number of different distributions of thickness.

Whether or not the resulting mean thicknesses are physically significant depends on whether other factors such as distortion broadening and thermal broadening are significant. A tape of draw ratio 25 annealed for 1 h at 129°C showed a slight increase in the (002) linewidth which suggests that distortion broadening is not present in the 'as-drawn' specimens. Measurements at -120°C showed no significant change in linewidth and we deduce from this that thermal broadening is not important at room temperature. Thus we conclude that our mean thicknesses are physically meaningful.

Small-angle scattering measurements

Small angle X-ray measurements were made using a Franks camera attached to a Siemens microfocussing X-ray tube. The scattering was recorded photographically and the long range repeat distance measured from the pattern on the film.

RESULTS

The apparent lattice modulus, E_c^{app} , as defined above, is shown in Figures 1 and 2 as a function of temperature for

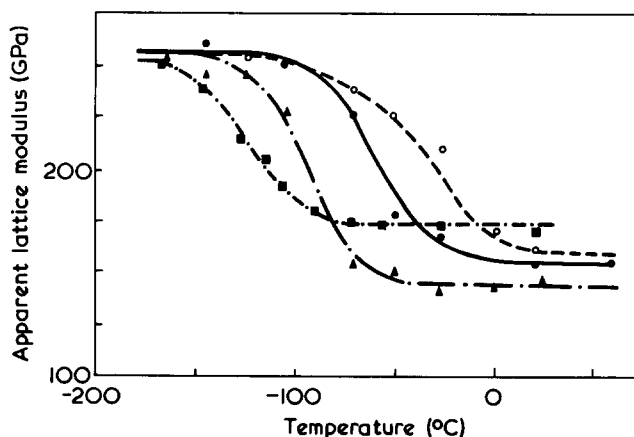


Figure 1 Apparent lattice modulus, E_c^{app} , as a function of temperature for three R50 samples of differing draw ratio (λ). Also shown, for comparison, are a set of results for a H020 sample. R50; \bullet , $\lambda = 9:1$; \blacktriangle , $\lambda = 19:1$; \blacksquare , $\lambda = 30:1$. H020; \circ , $\lambda = 10:1$

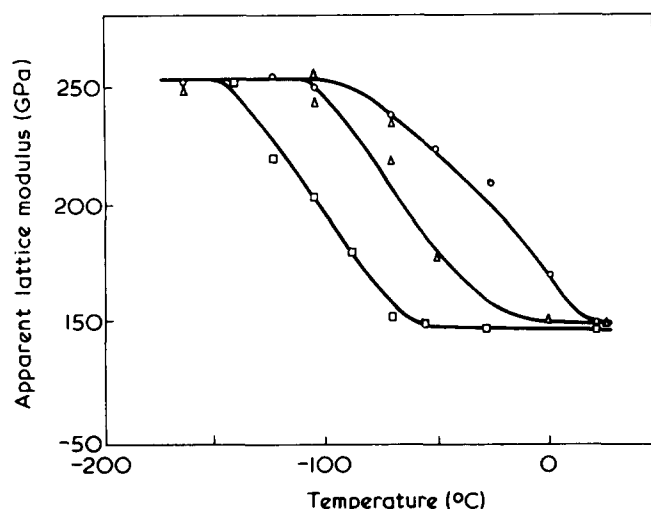


Figure 2 Apparent lattice modulus, E_c^{app} , as a function of temperature for three H020 samples of differing draw ratio (λ). \circ , $\lambda = 10:1$; \triangle , $\lambda = 15:1$; \square , $\lambda = 25:1$

different draw ratios and for the two different mean molecular weights used, (samples 1 and 2). The uncertainty in each point is of the order of 5 to 10 GPa, hence the curves show quite a consistent trend from room to low temperature.

A measurement was also made on a sample (sample 3) drawn to a ratio of 9 and which had been annealed at 129°C for 1 h. The apparent lattice modulus for this specimen has a value, at room temperature, close to that of the unannealed specimen at low temperature.

The most obvious feature of these results is that E_c^{app} rises to 255 ± 10 GPa in all specimens at low temperature. This would therefore seem to represent the ultimate Young's modulus of crystalline polyethylene if we make the quite reasonable assumption that at these low temperatures the non-crystalline fraction hardens to give uniformity of stress throughout the specimen. The stress on the crystalline fraction then equals the applied stress and $E_c^{\text{app}} = E_c^{\text{true}}$. At room temperature most specimens have $E_c^{\text{app}} \approx 150$ GPa and as will be seen later this figure enables an upper limit to be placed on the (X-ray) crystallinity of a sample.

Mean crystallite thicknesses in the three principal crystal directions a , b , and c (chain direction) are shown in Table 1 and indicate a constant thickness normal to the chain or fibre direction but a mean thickness which increases along the chain direction with increasing draw ratio. Long periods deduced from small-angle scattering are also shown and these remain more or less constant, but it should be noted that the scattered intensity falls off substantially as draw ratio increases, hence the regular 200 Å structure is still extant in the specimens but is less clearly defined at high draw ratios.

DISCUSSION

Orientation measurements made in this laboratory show that the crystalline chains are very highly aligned in all the samples used and the principal morphological differences between specimens of different draw ratio lie in the increased mean crystalline thickness in the 'c' direction with increased draw ratio.

This fact, together with the result of the small-angle studies suggest a systematic increase in crystal continuity in the chain direction with increasing draw ratio. In structural

terms this can be imagined as arising from the production of intercrystalline bridges as proposed by Fischer and coworkers⁷.

In the related paper on the mechanical properties of these ultra-high modulus drawn polymers⁴ it is shown that this concept of a change in the degree of crystal continuity can form the basis of a simple model which correlates quantitatively the mechanical stiffness and the measured crystal thickness in the (002) direction. In the present paper it is primarily of interest to gain an understanding of the crystal strain measurements. If possible, we would seek to avoid an explanation which is necessarily tied to a specific structural model because, as we will show, there is a generality in the results which can be understood without knowledge of the structure.

A very successful simple model which has proved valuable in understanding the mechanical behaviour of oriented crystalline polymers is that proposed by Takayanagi⁸. It has been shown that a Takayanagi model, modified to take into account the degree of crystal continuity, provides a satisfactory description at a phenomenological level for the low temperature Young's modulus and thermal conductivity of ultra-high modulus linear polyethylene⁹. This model, shown schematically in Figure 3 will now be shown also to give a satisfactory description of the crystal strain measurements.

It is important to recognize that there are in principle, two different ways of evaluating the modulus and the crystal strain on this model, depending on the assumptions which are made regarding continuity of strain and transfer of stress. On what we shall term the 'parallel-series' assumption, the material is regarded as an intercrystalline fraction (a) in series with the remaining crystalline fraction ($1 - a$), with the intercrystalline fraction containing a small parallel fraction (b) of intercrystalline bridges. The modulus in the draw direction E_{\parallel} is then given by:

$$\frac{1}{E_{\parallel}} = \frac{(1-a)}{E_C} + \frac{a}{bE_C + (1-b)E_a} \quad (1)$$

Table 1 Mean crystallite thicknesses in the three principal crystallographic directions and long periods in the 'c' direction for the various samples used. Also included are some measurements made on samples produced by the 'cold extrusion' process. The uncertainties in the crystal thickness measurements range from about 5% (for \bar{D}_{200} and \bar{D}_{020}) to 10% (for the larger values of \bar{D}_{002})

Sample	\bar{D}_{200} (Å)	\bar{D}_{020} (Å)	\bar{D}_{002} (Å)	Long period (Å ± 10Å)
R50 Draw ratio:				
9	102	112	240	185
19	101	113	410	190
30	105	108	464	198
H020 Draw ratio:				
10	131	121	271	256
15	125	118	362	262
25	125	118	520	266
30	128	123	554	262
H020 Draw ratio: (Annealed)				
Measured at 21°C	—	—	445	—
Measured at -120°	—	—	451	—
R50 Extruded Draw ratio:				
5.2	—	—	228	205
10.2	—	—	247	210
20	—	—	349	215

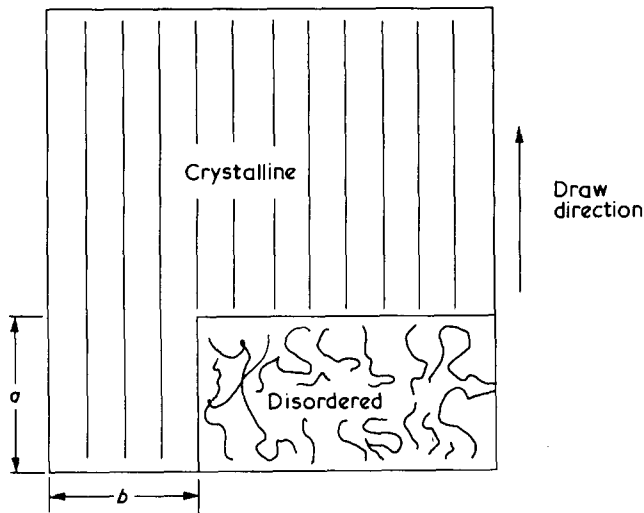


Figure 3 Schematic representation of the Takayanagi model referred to in the text

where E_C and E_a are the elastic moduli of the crystalline and disordered phase, respectively.

The average crystal strain $\bar{\epsilon}_c$ is:

$$\bar{\epsilon}_c = \frac{1}{\chi} \left[(1-a) + \frac{ab}{b + (1-b)E_a/E_c} \right] \epsilon \quad (2)$$

where $\chi = 1 - a(1-b)$ is the volume fraction of crystalline material and ϵ is the overall strain, and the apparent crystal modulus is given by:

$$\frac{E_c^{app}}{E_c} = \chi \left[(1-a) + \frac{ab}{b + (1-b)E_a/E_c} \right]^{-1} \quad (3)$$

We note that as $E_a \rightarrow 0$, $E_c^{app}/E_c \rightarrow \chi$ and that $E_c^{app} \rightarrow E_c$ as $b \rightarrow 0$ or $E_a \rightarrow E_c$. Furthermore it is always true that $\chi \leq E_c^{app}/E_c$.

It is also possible to consider the modified Takayanagi model on the 'series-parallel' assumption, the material now being regarded as a continuous crystalline fraction, b , in parallel with the remaining intercrystalline fraction, $(1-b)$, the latter containing a series fraction (a) of disordered phase. With this assumption the modulus in the draw direction, $E_{||}$, is given by:

$$E_{||} = E_c \left[b + \frac{(1-b)E_a/E_c}{a + (1-a)E_a/E_c} \right] \quad (4)$$

The average crystal strain $\bar{\epsilon}_c$ is now:

$$\bar{\epsilon}_c = \frac{1}{\chi} \left[b + \frac{(1-a)(1-b)E_a/E_c}{a + (1-a)E_a/E_c} \right] \epsilon \quad (5)$$

and the apparent crystal modulus is given by:

$$\frac{E_c^{app}}{E_c} = \frac{\chi \left[b + \frac{(1-b)E_a/E_c}{a + (1-a)E_a/E_c} \right]}{b + \frac{(1-a)(1-b)E_a/E_c}{a + (1-a)E_a/E_c}} \quad (6)$$

Again, it is to be noted that as $E_a \rightarrow 0$, $E_c^{app}/E_c \rightarrow \chi$ and that $E_c^{app} \rightarrow E_c$ as $b \rightarrow 0$ or $E_a \rightarrow E_c$. Again $\chi \leq E_c^{app}/E_c$, placing an upper limit on χ .

We can see that in spite of its simplicity the modified Takayanagi model does reproduce the principal features of the crystal strain results. Irrespective of the details of continuity of strain or stress transfer, E_c^{app} falls to the constant value χE_c as E_a falls, i.e. at high temperatures, and this result is independent of the degree of crystal continuity, represented by b on this model. We can also understand in general terms the draw ratio and molecular weight effects. For larger b , a correspondingly greater increase in E_a is required for E_c^{app} to rise. Thus in the higher draw ratio samples with larger degrees of crystal continuity the rise in E_c^{app} will occur at a lower temperature than for low draw ratio samples. The difference between samples of different molecular weight can be attributed to the more rapid fall in E_a with temperature for lower molecular weight samples, due to the more rapid decrease in internal viscosity with falling molecular weight. It is therefore reasonable to find that the fall in apparent modulus from E_c to E_c^{app} occurs at a lower temperature in the lower molecular weight samples for identical draw ratios.

An alternative model for the mechanical behaviour of an oriented polymer, which is also worthy of serious consideration, is the fibre composite model. It will be sufficient for our purposes in this paper to confine the discussion to broad generalities only. Following the well-known treatments of Cox and later workers¹⁰, the Young's modulus in the fibre direction of an aligned fibre composite is given by:

$$E_{||} = V_f \phi E_f + (1 - V_f) E_m \quad (7)$$

where V_f is the volume fraction of the fibre phase; E_f and E_m are the tensile modulus of the fibre and matrix, respectively, and ϕ is a parameter which allows for the 'ineffective length' at the end of a fibre where the stress decays (the shear lag effect). ϕ depends on the aspect ratio of the fibres and the shear modulus of the matrix, approaching unity as the aspect ratio becomes large and the shear modulus increases.

The average stress on the fibres is given by:

$$\sigma_f = E_f \phi \epsilon \quad (8)$$

where ϵ is the overall strain in the composite. The average strain in the fibres is then:

$$\bar{\epsilon}_f = \phi \epsilon \quad (9)$$

In the simplest application of the fibre composite model to an oriented polymer, the crystalline regions of the latter are identified as the fibre phase and the amorphous regions as the matrix. Equation (7) may then be written in terms of the quantities previously defined for the Takayanagi model, by putting $V_f = \chi$, $E_f = E_c$ and $E_m = E_a$. We have

$$E_{||} = \chi \phi E_c + (1 - \chi) E_a \quad (10)$$

an analogous equation to equations (8) and (9) for the average crystal stress and the average crystal strain.

The average crystal strain is:

$$\bar{\epsilon}_c = \phi \epsilon \quad (11)$$

and the apparent crystal modulus is given by:

$$\frac{E_c^{\text{app}}}{E_c} = \chi + \frac{1 - \chi}{\phi} \frac{E_a}{E_c} \quad (12)$$

It is interesting to note that the main features of the crystal strain data are again reproduced. Equation (12) shows that at high temperatures, provided that $E_a/E_c \rightarrow 0$ more rapidly than $\phi \rightarrow 0$, $E_c^{\text{app}}/E_c \rightarrow \chi$. We also note that $E_c^{\text{app}} \rightarrow E_c$ as $\phi \rightarrow 1$ and $E_a \rightarrow E_c$, which is a possible low temperature situation.

In this model, the increase in modulus with increasing draw ratio observed in ultra-high modulus polyethylenes is primarily attributed to the strong dependence of ϕ on draw ratio, in particular to an increase in the aspect ratio (which needs to be comparatively large) of the crystalline phase. The crystal thickness measurements, however, suggest much smaller aspect ratios than are required by the simple composite model. In the related paper on mechanical properties a statistical model is developed to describe the crystal continuity introduced by intercrystalline bridges. In this model the intercrystalline bridges stiffen the structure in a manner analogous to the reinforcing fibres in the fibre-reinforced composite. The model results in a quantitative expression for the Young's modulus of the drawn polymer which is exactly analogous to that for the fibre reinforced composite, but avoids the requirement of needle-like crystalline regions of high aspect ratio which are demanded by the simple composite model^{11,12}.

Although the statistical model is analogous to the fibre composite model, the fibre phase is now considered to be only the fraction of the crystalline phase which links the crystalline regions by intercrystalline bridges, and the matrix is a mixture of lamellar and disordered material. In terms of the parameters V_f and χ , V_f is less than χ and is a strong function of draw ratio. In this model, the fibres are considered to have a range of lengths, but in terms of the fibre composite model (equation 7), we can define an effective ϕ' such that:

$$E_{\parallel} = V_f \phi' E_c + (1 - V_f) E_m \quad (13)$$

If the matrix modulus E_m is calculated on the basis of series connectivity of the lamellar and disordered phase it may be shown that the result is equivalent to identifying V_f with the b of the 'series-parallel' modified Takayanagi model, but reducing b by the factor ϕ' .

The apparent crystal modulus is then given by:

$$\frac{E_c^{\text{app}}}{E_c} = \frac{\chi \left[V_f \phi' + \frac{(1 - V_f) E_a / E_c}{1 - \chi + (\chi - V_f) E_a / E_c} \right]}{\left[V_f \phi' + \frac{(\chi - V_f)(1 - V_f) E_a / E_c}{1 - \chi + (\chi - V_f) E_a / E_c} \right]} \quad (14)$$

Again, we see that as $E_a/E_c \rightarrow 0$, $E_c^{\text{app}}/E_c \rightarrow \chi$ and $E_c^{\text{app}}/E_c \rightarrow 1$ as $\phi' \rightarrow 1$ and $E_a \rightarrow E_c$.

A full account of this model is given in the related paper, where it is shown to reproduce the main features of the crystal strain data in some detail. Here we need only note that equations (13) and (14) bring together the modified Takayanagi model, the simple reinforced composite model, both of which are phenomenological, and the statistical model which relates to the crystal thickness measurements on the basis of a simplified model of the structure. Moreover, it has been

shown that a satisfactory general explanation of the crystal strain results from any of the equations (3), (6), (12) and (14) and is essentially model independent. Provided we hypothesize that there is some degree of crystal continuity, i.e. move away from the original Takayanagi-type model of crystalline and amorphous phases in series with no continuity of the crystalline phase, a simple explanation of the crystal strain data for the drawn tapes obtains. It is clearly an important observation that a room temperature measurement of E_c^{app} on an annealed sample of draw ratio 9 gave a value close to the low temperature value obtained with the other samples, a value which is believed to be E_c . At the same time a considerable increase in the intensity of the two point small-angle X-ray diffraction pattern was observed. These results are consistent with this material possessing a simple parallel lamellar texture. Extensive mechanical measurements on such samples¹³ led to the conclusion that there was no crystal continuity in this case.

These theoretical considerations provide justification for the conclusion that E_c^{app}/E_c at high temperatures provides a definitive upper limit for χ , the volume fraction of crystalline material. It is to be noted that the values obtained in this way for χ are ~ 0.6 , which are much less than those estimated from density, d.s.c. and broad line nuclear magnetic resonance where values ~ 0.8 are typically obtained. This suggests that a substantial part of the material which does not contribute to the X-ray diffraction pattern is nevertheless very appreciably ordered. It seems likely that the molecular chains are aligned without possessing three-dimensional order over a sufficiently large volume. An appreciable degree of order in the non-crystalline material is consistent with our second general conclusion. This is that at low temperatures $E_c^{\text{app}} \rightarrow E_c$ because E_a (or E_m in the fibre composite model) rises to a value which is now comparable with E_c . Thus, both our principal conclusions argue for an ordered 'amorphous' phase.

CONCLUSION

X-ray measurements on high modulus polyethylene fibres have indicated a structure rather different from that of a simple composite. The structure is more continuous in nature and it is easier to visualize its development as the drawing process progresses than in the case of a simple composite. In essence the structure is a kind of compromise between a lamellar model and an extended-chain model and, in the nature of such complex materials, as polymers, it is perhaps not surprising that such a compromise is a good description of the physical reality.

REFERENCES

- 1 Capaccio, G. and Ward, I. M. *Nature Phys. Sci.* 1973, **243**, 143; *Polymer* 1974, **15**, 233
- 2 Capaccio, G., Crompton, T. A. and Ward, I. M. *J. Polym. Sci. (Polym. Physics Edn)* 1976, **14**, 1641
- 3 Gibson, A. G., Ward, I. M., Cole, B. N. and Parsons, B. *J. Mater. Sci.* 1974, **9**, 1193
- 4 Gibson, A. G., Davies, G. R. and Ward, I. M. *Polymer* 1978, **19**, 683
- 5 Britton, R. N., Jakeways, R. and Ward, I. M. *J. Mater. Sci.* 1976, **11**, 2057
- 6 Stokes, A. R. *Proc. Phys. Soc. (London)* 1948, **61**, 382

Ultra-high modulus linear polyethylene: J. Clements et al.

- | | | | |
|---|--|----|--|
| 7 | Fischer, E. W., Goddar, H. and Peiszczek, W. <i>J. Polym. Sci. (C)</i> 1971, 32 , 149 | 10 | Cox, H. <i>Br. J. Appl. Phys.</i> 1952, 3 , 72 |
| 8 | Takayanagi, M., Imada, K. and Kajiyama, T. <i>J. Polym. Sci. (C)</i> 1966, 15 , 263 | 11 | Arridge, R. G. C., Barham, P. J. and Keller, A. <i>J. Polym. Sci. (Polym. Phys. Edn)</i> 1977, 15 , 389 |
| 9 | Gibson, A. G., Greig, D., Sahota, M., Ward, I. M. and Choy, C.L. <i>J. Polym. Sci. (Polymer Letters Edn)</i> 1977, 15 , 183 | 12 | Gibson, A. G. <i>PhD Thesis</i> , Leeds University, UK (1977) |
| | | 13 | Kapuscinski, M., Ward, I. M. and Scanlan, J. <i>J. Macromol. Sci. (B)</i> 1976, 11 , 475 |